Published in final edited form as:
Dev Biol. 2010 May 1; 341(1): 176–185. doi:10.1016/j.ydbio.2010.02.025.

CACN-1/Cactin interacts genetically with MIG-2 GTPase signaling to control distal tip cell migration in *C. elegans*

Hiba Tannoury[1], **Varenka Rodriguez**[1], **Ismar Kovacevic**[1], **Mouna Ibourk**[1], **Myeongwoo Lee**[2], and **Erin J. Cram**[1,*]

[1] Department of Biology, Northeastern University, 360 Huntington Ave, 134 Mugar Hall, Boston, MA, 02115

[2] Department of Biology, Baylor University, One Bear Place 97388, Waco, TX 76798

Abstract

The two specialized *C. elegans* distal tip cells (DTCs) provide an *in vivo* model system for the study of developmentally regulated cell migration. We identified *cacn-1*/*cactin*, a well-conserved, novel regulator of cell migration in a genome-wide RNAi screen for regulators of DTC migration. RNAi depletion experiments and analysis of the hypomorphic allele *cacn-1(tm3126)* indicate that CACN-1 is required during DTC migration for proper pathfinding and for cessation of DTC migration at the end of larval morphogenesis. Strong expression of CACN-1 in the DTCs, and data from cell-specific RNAi depletion experiments, suggest that CACN-1 is required cell-autonomously to control DTC migration. Importantly, genetic interaction data with Rac GTPase activators and effectors suggest that CACN-1 acts specifically to inhibit the *mig-2*/Rac pathway, and in parallel to *ced-10*/Rac, to control DTC pathfinding.

Keywords

Cactin; cell migration; Rac; GTPase; gonad; distal tip cell; *C. elegans*

Introduction

Cell migration is of fundamental biological importance. It is essential for embryonic development during tissue and organ morphogenesis, and for immune system function and wound healing in the adult. Mechanisms of cell migration, including regulation of integrin-containing adhesion complexes, Rac family GTPases, and the acto-myosin contractile machinery, are conserved throughout evolution (Heasman and Ridley, 2008; Lehmann, 2001). The invariant pattern of cell migration, translucent body, and availability of cell-specific GFP markers make *C. elegans* an ideal model system with which to dissect the molecular basis of cell migration. Studies of axon guidance (Killeen and Sybingco, 2008), sex myoblast migration (Chen and Stern, 1998) and distal tip cell (DTC) migration (Kimble and Hirsh, 1979; Lehmann, 2001; Nishiwaki, 1999) have all helped to reveal the mechanisms by which migrating cells adhere to extracellular matrix (ECM) molecules, interpret guidance cues, and coordinate cell movements with embryonic and larval stages. Despite these advances, much

*All correspondence should be addressed to: Erin Cram, Ph.D., Telephone: (617) 373–7533, Fax: (617) 373–3724, e.cram@neu.edu.

remains to be learned about how migrating cells integrate multiple inputs and coordinate cytoskeletal and signaling proteins to influence cell polarity and generate directed cell motility.

Gonad morphogenesis in *C. elegans* is dependent on the migration of a specialized leader cell, the distal tip cell (Lehmann, 2001). During the four stages of larval development (L1, L2, L3, and L4), the DTC migrates in response to attractive and repulsive cues to properly form the mirror image U-shaped gonad (Lehmann, 2001). Conserved guidance systems control DTC migration, including cues such as UNC-129/TGF-β (Colavita et al., 1998), UNC-6/netrin (Merz et al., 2001), and integrin signaling (Lee et al., 2001; Meighan and Schwarzbauer, 2007). These signals impinge upon the Rac GTPases (Levy-Strumpf and Culotti, 2007; Lundquist et al., 2001) which regulate actin and microtubule cytoskeletal organization, orientation, and stabilization, thereby influencing cell migration and pathfinding (Hall, 2005). GTPases are activated by guanine nucleotide exchange factors (GEFs) that stimulate exchange of GDP for GTP and are inhibited by GTPase activating proteins (GAPs) that stimulate the hydrolysis of GTP (Rossman et al., 2005). In *C. elegans*, the GTPases CED-10, MIG-2 and RAC-2 and the UNC-73 GEF are required for the migration of a variety of axons and cells, including the distal tip cell (DTC) (Lundquist, 2003; Lundquist et al., 2001; Reddien and Horvitz, 2000; Zipkin et al., 1997). The underlying molecular mechanism involves linking the proteins that mark the direction of polarization to the cytoskeletal changes that reinforce it and allow directional cell migration.

In order to further elucidate the mechanism of DTC migration, we conducted a genome-wide RNA interference screen and evaluated the migration of the DTCs using light microscopy (Cram et al., 2006). In addition to known regulators of cell migration, this study identified several novel regulators of cell migration, including CACN-1. CACN-1 is the homolog of *Drosophila* Cactin, a protein that interacts with Cactus/IKB and functions in the Rel/NFKB pathway to control the formation of dorsal-ventral embryonic polarity in fly (Lin et al., 2000). Cactus/IKB is found in a cytoplasmic complex with Dorsal/NFKB. Degradation of Cactus frees Dorsal to translocate to the nucleus and regulate transcription of target genes. Cactin is thought to promote nuclear targeting of Dorsal/NFKB by destabilizing Cactus/IKB. CACN-1 is very well conserved from nematodes to humans, but little is known about its molecular function in any organism. Previous to this work nothing was known about its function as a regulator of cell migration.

In this study we demonstrate that CACN-1 is required for correct DTC migration and for gonad morphogenesis. We characterize two deletion alleles, one of which is a weak hypomorph that exhibits gonad defects similar to those seen in *cacn-1* RNAi. The DTC requires CACN-1 for accurate pathfinding, for cessation of migration, and for the control of final gonad size. We present genetic evidence that suggests *cacn-1* interacts genetically with the Rac GTPase *mig-2* to regulate distal tip cell pathfinding.

Materials and methods

Nematode strains

Nematodes were cultivated on NGM agar plates with *E. coli* OP50 bacteria according to standard techniques (Brenner, 1974). Nematode culture and observations were performed at 23 degrees, unless otherwise indicated. The following strains were used for these studies: N2 (wild type reference strain, Bristol), *cacn-1(tm3042)* and *cacn-1(tm3126)* (from Shohei Mitani and the Japanese National Bioresource Project, Tokyo, Japan), the UN0701 xbEx0701 [*900cacn-1*::GFP], the NK598 *unc-119(ed4)*; qyIs96[*5300cacn-1*::GFP, *unc-119*(+)], and the NK599 *unc-119(ed4)*; qyIs97 [*5300cacn-1*::GFP, *unc-119*(+)] transcriptional fusion lines (NK strains are a gift of David Sherwood, Duke University, Durham, NC, USA), the DTC expression translational fusion line UN0956 xbEx0956[*lag-2::cacn-1*::GFP, *rol-6* (pRF4)],

the MIG-2::GFP expression line CF693 *unc-31(e169); him-5(e1490)*; muIs28[MIG-2::GFP + *unc-31*(+)], the CED-10::GFP expression line MT10865 *unc-76(e911)*; nEx1039[p-*ced-10*::GFP::CED-10 + *unc-76*(+)], the SP127 *unc-4(e120); mnC1 dpy-10(e128), unc-52 (e444)* balancer strain for balancing *cacn-1(tm3042)* in strain UN0705, the UN0938 *cacn-1 (tm3042)*; xbEx0938[*cacn-1*(+), *sur-5*::GFP], and UN0951 *cacn-1(tm3126)*; xbEx0938 [*cacn-1*(+), *sur-5*::GFP] genomic rescue strains, the NL2099 *rrf-3(pk1426)* RNAi sensitive strain, the CF162 *mig-2(mu28)* null allele, the NG103 *mig-2(gm103)* gain of function allele, the MT4434 *ced-5(n1812)* and MT4952 *ced-2(n1994)* null alleles, the MT5013 *ced-10 (n1993)* hypomorph and the heterozygous null MT10869 *ced-10(n3417); lin-1(e1275), dpy-13 (e184)*, the DV2078 *pak-1(ok448)*, DV2138 *pak-1(tm403)*, and DV2202 *max-2(nv162)* putative null alleles, and the DV2283 *max-2(cy2)* hypomorphic allele (DV strains provided by Dave Reiner, University of North Carolina, Chapel Hill, USA), the UN0802 *rde-4(ne301);* xbEx0802[*lag-2*::RDE-4::GFP, *rol-6* (pRF4)] DTC-specific RNAi strain, UN0907 *rde-4 (ne301)* xbIs20[*vha-6*::RDE-4::GFP, *unc-119(+)*] intestinal-specific RNAi strain, and the RNAi-deficient strain WM49 *rde-4(ne301)*.

Transgenic animals

In order to generate UN0701 *cacn-1*::GFP nematodes, nucleotide sequences upstream of the *cacn-1* translational start (−1 to (−900) were amplified from N2 genomic DNA using PCR and cloned into the HindIII and BamHI sites of the GFP expression vector pPD95_77 (provided by Andrew Fire, Stanford University, Palo Alto, CA, USA) to generate the *cacn-1*::GFP reporter. In order to generate UN0956 lag-2::*cacn-1*::GFP nematodes, lag-2 promoter sequences were amplified from pJK590 lag-2::GFP (gift of Judith Kimble, University of Wisconsin, Madison, USA) using PCR and cloned into the HindIII and PstI sites of the cacn-1::GFP vector described above. Extrachromosomal arrays were generated by germline transformation of N2 animals with *cacn-1*::GFP DNA (50 μg/ml) and stable chromosomal integration was induced by treatment with UV. The rescued line UN0938 was generated by micro-injecting the UN0705 strain with the *cacn-1* genomic region amplified from genomic DNA using Expand Long-range dNTPack (Roche). The forward primer 5′ was designed to anneal 913 bp upstream of the translational start, and the reverse primer was designed to anneal 793 bp downstream of the translational stop (all primer sequences available upon request). The 10249 bp amplicon was agarose gel purified using the Zymoclean Gel DNA Recovery Kit (Zymo Research, Orange, CA, USA). Transgenic nematodes were generated by microinjection of the purified PCR product at a concentration of approximately 50 ng/μl into the UN0705 strain with a co-injection of approximately 50 ng/μl pTG96 (*sur-5*::GFP). The rescued strain UN0938 was isolated by singling out green F1 progeny and selecting those that lacked dumpy and uncoordinated F2 progeny. UN0938 produces fertile green *cacn-1(tm3042);* [*cacn-1*(+), *sur-5*::GFP] progeny and arrested non-green *cacn-1(tm3042)* progeny. The rescued line UN0951 was generated by crossing cacn-1(tm3126) homozygous animals with N2 animals carrying the genomic xbEx0938[*cacn-1*(+), *sur-5*::GFP] extrachromosomal array. F2 animals homozygous for cacn-1(tm3126) were isolated and verified by genomic PCR.

In RNAi-deficient *rde-4(ne301)* mutant animals, a functional RDE-4::GFP fusion protein is expressed under control of the cell-type-specific promoter, thereby rescuing RNAi function in that cell type only. In order to generate the UN0802 DTC-specific RNAi strain, the 3204 bp *lag-2* promoter was amplified from the pJK590 vector (gift of Judith Kimble, University of Wisconsin, Madison, USA) using PCR and cloned into the HindIII and BamHI sites of the pPD95_75GTWY vector (gift of Barth Grant, Rutgers University, Piscataway, NJ, USA). The *rde-4* open reading frame was amplified from clone T20G5.11 (Open Biosystems, Huntsville, AL, USA) with primers containing a start codon and L1/L2 recombination sites, and LR Clonase (Invitrogen) was used to insert *rde-4* sequences into pPD95_75GTWY. In order to generate the UN0907 intestinal-specific RNAi strain, the *rde-4* open reading frame flanked

with L1/L2 recombination sites was recombined into the *vha-6p*::GFP GTWY vector (gift of Barth Grant, Rutgers University, New Brunswick, NJ, USA). The integrated line OX306 (gift of Martha Soto, UMDNJ, Piscataway, NJ, USA) was generated by biolistic transformation of the array [*vha-6*::RDE-4::GFP, *unc-119(+)*] into *unc-119(ed4)* animals. UN0907 was generated by crossing OX306 into *rde-4(ne301)* animals. Correct expression pattern was confirmed using GFP epifluorescence.

RNAi

Starved nematodes were allowed to recover on fresh OP50 seeded NGM plates for two days. This procedure produces gravid young adult hermaphrodites for egg collection. Eggs were released using alkaline hypochlorite solution (Hope, 1999). Following two washes in M9 buffer, eggs were transferred to plates seeded with RNAi HT115(DE3) bacteria expressing dsRNA. If more closely synchronized progeny groups were required, hermaphrodites were allowed to lay eggs directly on the seeded RNAi plates for one hour, and then removed using a vacuum. The nematode strain used in each experiment is indicated. For most experiments, N2 or *rrf-3(pk1426)* strains were used. For cell type-specific RNAi, UN0802 and UN0803 strains were compared to N2 and to the RNAi resistant WM49 strain.

The RNAi feeding protocol was essentially as described (Timmons, 2006). Briefly, bacteria were cultured overnight in LB supplemented with 40 μg/ml ampicillin and seeded onto NGM agar supplemented with carbenicillin (25 μg/ml) and IPTG (1mM). Double-stranded RNA expression was induced overnight at room temperature on the IPTG plates. Eggs were then transferred onto the plates and the RNAi phenotypes were monitored at the times indicated.

The *cacn-1* ORF RNAi clone is a full-length cDNA matching WormBase (WS200) predictions (Open Biosystems, Huntsville, AL, USA). The 5′ *cacn-1* RNAi clone is a 425 bp fragment of *cacn-1* cloned into the RNAi feeding vector pPD129.36. Primers at positions 205 and 630 relative to the ATG in the predicted cDNA sequence were used for RT-PCR amplification of N2 total RNA as the template. Primers included NheI and HindIII sites at the 5′ and 3′ ends respectively, and were used to clone the PCR product into pPD129.36. The 3′ *cacn-1* RNAi clone is a genomic clone from well II9E09 of the Ahringer RNAi library (Kamath et al., 2003).

Analysis of phenotypes

To analyze gonad morphology, partially synchronized populations of animals were mounted in a drop of M9 containing 0.08M sodium azide on a slide coated with 2% agarose in water and examined using a Nikon 80i microscope with DIC optics. DTC migration defects were inferred from the resulting shape of the gonad arms. Defects such as insufficient distance migrated along the ventral surface, inappropriate or extra turns, and failure to cease migrating at the vulva were counted as DTC migration defects. Distances traveled in each phase of DTC migration were quantified using Spot Advanced software version 4.6.4.6. All proportions were compared for statistical differences by calculating binomial 95% confidence intervals using JavaStat. Medians in the gonad growth study were compared with the Mann Whitney statistic using GraphPad Prism statistical software.

Results

CACN-1 gene structure and deletion alleles

CACN-1 is very well conserved. The conservation to human cactin (C19ORF29), a renal tumor antigen (Scanlan et al., 1999) has a BLAST E-value of 5e-118 for alignment over 99.7% of the length of the protein. This corresponds to ~70% similarity and 40% identity of the 677 amino acid sequence. The cactin C-terminus features a block of 52 amino acids >90% identical

between the fly, worm, and human sequences (Lin et al., 2000). CACN-1 protein has a putative nuclear localization signal at the N-terminus, central coiled-coil domains that may mediate protein interactions and a highly conserved C-terminus of unknown function. Sequencing of *cacn-1* cDNAs produced by RT-PCR from N2 total RNA and sequencing of a selection of W03H9.4 open reading frame (ORF) clones purchased from Open Biosystems show that the WormBase (Chen et al., 2005) gene model for *cacn-1* is almost entirely correct. The single difference we reproducibly find is a mis-prediction of the intron 5 splice site that results in a replacement of the predicted sequence 452RFSIFFLAEKP462 with 452S. This sequence is not in a well-conserved portion of the predicted protein.

We obtained two *cacn-1* deletion alleles, *tm3042* and *tm3126*, from the Japanese National Bioresource Project. The *tm3042* allele is a 182 bp deletion near the 5′ end of the gene and results in a frame shift (Fig. 1). The predicted protein product has a substitution of 14 amino acids (117FASRRQGRHGNDET130 for amino acids 117KSGLTQDEITKQTS130) and is truncated after the 130th amino acid. In order to maintain *tm3042*, we have constructed strain UN0705 by crossing heterozygous *tm3042* animals with SP127, a strain containing the well characterized balancer *mnC1(II)*(Edgley et al.). Self-progeny of *tm3042*/+ heterozygous mothers include viable and fertile +/+ and *tm3042*/+ animals and *tm3042/tm3042* homozygotes that variably arrest as L1 and L2 larvae. The larval arrest phenotype precludes the analysis of the role of *cacn-1* in DTC migration using this allele. Although wild type cDNA can readily be detected, we have been unable to detect *tm3042* specific cDNA in *tm3042*/+ or UN0705 heterozygotes, suggesting the message is unstable and likely not translated (data not shown). In addition, we have been unable to detect *cacn-1* message in *tm3042* arrested larvae using single worm RT-PCR. These results suggest *cacn-1(tm3042)* is a probable molecular null allele. A 10 kb genomic DNA from the *cacn-1* locus, including a 900 bp promoter region and 800 bp of 3′ sequence, is sufficient to completely rescue the larval arrest of *cacn-1(tm3042)*.

Animals homozygous for the second allele, *tm3126*, exhibit much milder phenotypes. The *tm3126* allele is a 162 bp in-frame deletion of part of the second exon, the second intron, and part of the third exon (Fig. 1). The *tm3126* cDNA can easily be detected, and has been sequenced to confirm the deletion. The predicted affect on the protein is a missense mutation E113D, and a deletion of 25 amino acids (R114-H138). The *tm3126* homozygous animals are viable and fertile, but exhibit defects in gonad morphogenesis (described below).

CACN-1 is expressed in the pharynx, intestine, vulva, germline and somatic gonad

In order to determine which tissues express CACN-1, nematode lines expressing *cacn-1*::GFP were generated. Several attempts to establish a nematode line expressing a CACN-1::GFP fusion protein resulted in abnormal animals that failed to transmit the transgene to progeny, possibly due to a deleterious overexpression phenotype of the GFP fusion protein. We therefore prepared transgenic animals expressing GFP under the control of 900 bp of genomic sequence 5′ of the predicted CACN-1 translational start site. This is the entire intragenic region between W03H9.3 and W03H9.4, and it corresponds to the promoter used in the rescuing genomic fragment. Fluorescence microscopy of integrated UN0701 *cacn-1*::GFP transgenic animals shows that GFP is expressed broadly in larval and adult animals, including strong expression in the pharynx, intestine, vulva, germline and cells of the somatic gonad including the spermatheca, gonad sheath, and DTC. GFP is expressed in migrating DTCs throughout larval development and persists into adulthood. We compared the UN0701 *cacn-1*::GFP animals to two transgenic nematode lines expressing GFP under the control of 5300 bp of 5′ *cacn-1* sequence (NK598 and NK599) and found a similar expression pattern (Fig. 2). In order to determine the subcellular localization of CACN-1, we generated animals that express a CACN-1::GFP fusion protein in the DTC under the control of the *lag-2* promoter. In these animals, we observed a nuclear and cytoplasmic distribution of CACN-1:GFP in the DTC (Fig

2D). Therefore, CACN-1 appears to be expressed at the right time and place to control DTC migration in the larval animal.

CACN-1 is required for correct DTC pathfinding

The gene *cacn-1* was identified in our genome wide RNAi screen for *C. elegans* genes involved in DTC migration (Cram et al., 2006). During normal *C. elegans* development, migration of the DTC guides the formation of the hermaphrodite gonad (Lehmann, 2001). During the four stages of larval development (L1, L2, L3, and L4), the DTC radically changes direction exactly two times, in response to attractive and repulsive cues, to properly form the mirror image U-shaped gonad (Lehmann, 2001). The two DTCs are easily visible in the living worm, and the shape of each gonad arm reflects the migratory path taken by the DTC during larval development. If the DTC fails to migrate or follows an aberrant path, malformation of the gonad arm will result (Fig. 3).

One prominent phenotype in *cacn-1* RNAi animals is that the DTC does not stop migrating at the correct position, commonly overshooting the midline (Fig. 3B and Table 1). Quantitative analysis of the distance from the vulva to the DTC indicates that by 72 hours post egg-prep, *cacn-1* RNAi DTCs have migrated much further past the midline than DTCs in control animals (Fig. 4). In the majority of animals, migration of the DTC during L4 is essentially normal (Supplementary Fig. S1). In control animals the DTC stops migrating by the end of L4 and is correctly positioned at the vulva. In animals treated with *cacn-1* RNAi, the DTC migrates throughout L4 and continues migrating during adulthood. In extreme cases, the DTC stops migrating when it can not squeeze its way past the pharynx. We observed the position of the DTC in individual animals at the end of L4 (48 hours), recovered the animals on control or *cacn-1* RNAi food, and then observed the same animal again one day later in young adulthood (72 hours). During this time frame, the DTC in control animals does not migrate, but in *cacn-1* RNAi treated animals, the DTC continues to migrate, moving an average of 125 +/− 79 μm (N=7). Comparison of control RNAi and *cacn-1* RNAi treated animals demonstrated that loss of *cacn-1* also causes other significant defects in DTC migration including wandering and inappropriate extra turns (Table 1). Importantly, similar results were obtained using two non-overlapping *cacn-1* RNAi targeting constructs and defects were rarely observed in animals fed control RNAi bacteria (Table 1). Another gene, K09E4.1, is expressed from sequences overlapping the *cacn-1* locus. Animals fed RNAi clones targeting K09E4.1 had no DTC migration or other apparent defects (data not shown). These results suggest DTC migration defects are specific to knockdown of *cacn-1*.

The *cacn-1(tm3126)* animals also exhibit defects such as failed DTC migration, mild pathfinding defects, and extra turns (Table 1). This result suggests either that the N-terminal sequences deleted in *cacn-1(tm3126)* are required for correct DTC migration, or that the *tm3126* deletion may destabilize the protein structure leading to sporadic loss of *cacn-1* function. However, DTCs in *tm3126* animals do not overshoot the midline, implying that *tm3126* retains sufficient function to convey stopping information to the DTC. Given these results, we predicted that *tm3126* acts as a weak hypomorph. To test this idea, we crossed the *cacn-1(tm3126)* animals with the *cacn-1(tm3042)* UN0705 balanced line. F1 trans heterozygotes are viable and fertile and display mild DTC migration defects suggesting *cacn-1 (tm3126)* retains significant function. As expected, *tm3126/tm3042* animals have a significantly higher percentage of DTC migration defects than *tm3126* homozygotes or *tm3042*/+ heterozygotes (Table 1). In addition, *cacn-1(tm3126)* animals treated with *cacn-1* RNAi exhibit more severe and penetrant DTC migration defects than *cacn-1(tm3126)* control treated animals (Fig. 3 and Table 1). Often, the DTCs fail to migrate completely, and short gonad arms result (Fig. 3E). In order to determine if this increased severity is attributable to *tm3126*, we established *tm3126* rescued nematodes over-expressing wild type *cacn-1*. When

treated with *cacn-1* RNAi, rescued animals display normal DTC migration (7% abnormal DTC migration, N=40), most likely because overexpression of wild type CACN-1 prevents efficient knockdown. In contrast, non-rescued *tm3126* siblings treated with *cacn-1* RNAi display the expected DTC migration defects (78% abnormal DTC migration, N=54). These results indicate that the severe DTC migration defects in *tm3126* treated with *cacn-1* RNAi are due to *tm3126* and not to another closely linked mutation, and suggest that *cacn-1* may be required cell autonomously to regulate DTC migration. We suspect the protein encoded by *cacn-1 (tm3126)* is less stable or expressed at lower levels than wild type CACN-1, making the product easier to deplete by RNAi.

CACN-1 is required for the gonad to achieve the proper adult size

During our initial characterization of *cacn-1* related phenotypes, we consistently observed that gonads in *cacn-1* RNAi treated animals were insufficiently elongated along the ventral body wall muscle, and much skinnier than normal (Fig. 3B). We measured the distance from the vulva to the first turn in control and *cacn-1* RNAi treated adult animals at a time point 72 hours after hatching. This analysis indicates that the length of the gonad along the ventral side in *cacn-1* RNAi treated animals is only half that of control animals (Fig. 5A). The severity of this *cacn-1* RNAi phenotype is similar in N2 and RNAi sensitive *rrf-3* animals.

We speculated that DTC migration defects might account for the short appearance of the gonad arms. For example, the DTC could turn away from the ventral side too early due to hypersensitivity to a repulsive cue, or might migrate too slowly. Alternatively, defects in the overall growth of the gonad could result in the apparent insufficient gonad elongation seen in young adult animals. In order to distinguish between these two explanations, we measured the length of the gonad arms at the point at which the DTC turns from the ventral toward the dorsal side (Fig. 5C). In *rrf-3* animals treated with control RNAi, the length of the gonad at the time of the first turn was 234 +/− 20 μm (body length 612 +/− 17 μm). Surprisingly, the *cacn-1* RNAi treated animals did not differ significantly from control RNAi treated animals at this time point. In *cacn-1* RNAi treated animals, the length of the gonad at the time of the first turn was 237 +/− 28 μm (body length 625 +/− 12 μm). To further characterize this phenotype, we measured gonad lengths along the ventral surface in N=200 larval and young adult animals. This gonad length data was then grouped by developmental stage, which was determined using the time elapsed since hatching, body length, and development of the vulva. A statistically significant difference in the median gonad length between control and *cacn-1* RNAi treated populations was only observed in the L4 and young adult animals (Fig. 5B). Therefore, the gonad morphogenesis defect in *cacn-1* RNAi treated animals becomes significant only after DTC migration is essentially complete. These results indicate that DTC migration per se along the ventral surface is not affected by *cacn-1* RNAi depletion in N2 animals, and suggest that defects in organ growth contribute more significantly than DTC migration to the observed differences in final gonad size.

CACN-1 is required cell-autonomously for correct gonad morphogenesis

In order to further determine if CACN-1 is required cell-autonomously to control DTC migration, we used a cell-specific RNAi approach. Cell-specific RNAi has the important advantage that the effect of RNAi can be limited to a specific tissue, and genes with lethal defects when systemically depleted can be studied using this approach (Qadota et al., 2007). To perform cell-specific RNAi, RNAi-deficient *rde-4(ne301)* mutant animals were transformed with a functional RDE-4::GFP fusion protein expressed under control of a cell-type specific promoter, thereby rescuing RNAi function in that cell type only. The *rde-4 (ne301)* animals are unaffected by *cacn-1* RNAi and have normal gonad elongation (Table 2). Using *gon-1* RNAi, which produces a striking and highly reproducible DTC migration defect, we verified that genes can be effectively silenced in the DTC-specific RNAi animals (*rde-4*

(ne301); [*lag-2*::RDE-4::GFP]) (Table 2). In contrast, when the intestinal cell-specific (*rde-4 (ne301);* [*vha-6*::RDE-4::GFP]) animals are treated with *gon-1* RNAi, no DTC migration defects are observed (Table 2). This suggests that there is very little spreading of RNAi from the intestine to non-target tissues. When treated with *cacn-1* RNAi, *rde-4(ne301);* [*lag-2*::RDE-4::GFP] animals exhibit DTC migration and vulval defects. The vulval defects are most likely due to the expression of *lag-2* transgenes in cells descended from Z1 and Z4 including the anchor cell (Kimble and Hirsh, 1979). Importantly, *rde-4(ne301);* [*lag-2*::RDE-4::GFP] animals displayed the characteristic overshoot phenotype associated with loss of *cacn-1* function in N2 and *rrf-3* animals (Fig. 6). In contrast, when the *rde-4 (ne301);* [*vha-6*::RDE-4::GFP] animals were treated with *cacn-1* RNAi, no DTC defects were observed (Table 2). These results suggest that *cacn-1* is required within the DTC to control DTC migration.

CACN-1 interacts genetically with the Rac GTPases to control DTC pathfinding

The DTC pathfinding defects seen in *cacn-1(tm3126)* and *cacn-1* RNAi animals are similar to those caused by disruption of Rac signaling (Lundquist et al., 2001). Therefore, we hypothesized that CACN-1 might be working through Rac GTPases to control DTC guidance. The adaptor *ced-2*/CrkII and the GEF *ced-5*/DOCK180 act upstream of the Rac GTPases *mig-2* and *ced-10* to control DTC migration (Lundquist et al., 2001). In order to investigate the genetic interaction between *cacn-1* and these upstream components, we treated mutant animals expressing null alleles *ced-2(n1994),* and *ced-5(n1812)* with *cacn-1* RNAi. The distal tip cell pathfinding defects in *ced-2(n1994)* and *ced-5(n1812)* animals were not enhanced by *cacn-1* RNAi (Table 3). This may suggest that *cacn-1* works in the same pathway as *ced-2* and *ced-5* to control DTC pathfinding.

In order to investigate the genetic interaction between *cacn-1* and Rac GTPases, we treated mutant animals expressing a strong loss of function allele *ced-10(n1993),* and two different null alleles of *mig-2, mig-2(mu28)* and *mig-2*(*gm38mu133),* with *cacn-1* RNAi. The loss-of-function *ced-10(n1993)* was used preferentially because *ced-10(n3417)* null is a maternal effect lethal allele (Lundquist et al., 2001). Both of these *ced-10* mutant animals have similar DTC migration defects (Lundquist et al., 2001). We found that *cacn-1* RNAi strongly enhanced the *ced-10(n1993)* phenotype, resulting in an increased penetrance and severity of pathfinding defects. In contrast, neither the *mig-2(mu28)* nor the *mig-2*(*gm38mu133)* DTC pathfinding defect was enhanced by *cacn-1* RNAi (Table 3). We also tested the genetic interaction between *ced-10* and *cacn-1* by treating the progeny of *ced-10 (n3417/+)* animals with *cacn-1* RNAi. Wild type F1 progeny could be distinguished by the dumpy phenotype conferred by the *dpy-13 (e184)* allele marking the wild type *ced-10* chromosome. Analysis of DTC migration defects in the remaining heterozygous and *n3417* homozygous F1 animals indicates loss of a single copy of *ced-10* strongly sensitizes the DTC to loss of *cacn-1* (Table 3). Since it is not possible to score DTC migration phenotypes in animals completely devoid of CED-10, the possibility that *cacn-1* might work in the same pathway as *ced-10* cannot be ruled out. These results suggest *cacn-1* is working in the same pathway as *mig-2*/Rac, *ced-2*/CrkII, and *ced-5*/DOCK180, and either in the same pathway or parallel to *ced-10*/Rac to control DTC migration.

We then tested the Rac effectors *pak-1* and *max-2* for genetic interactions with *cacn-1*. These two p21 activated kinases (PAK) are redundant for the control of DTC migration (Lucanic and Cheng, 2008), and have low penetrance DTC migration defects on their own. DTC pathfinding defects in both *pak-1(ok448)* and *pak-1(tm403),* and to a greater extent *max-2(nv162)* and *max-2(cy2),* are strongly enhanced by loss of *cacn-1*, suggesting that *cacn-1* works in parallel to *pak-1* and *max-2* to control DTC migration (Table 3).

In *cacn-1* RNAi animals, the DTC commonly fails to stop migrating at the correct point, far overshooting the midline (Fig. 3 and Fig. 4). During our genetic interaction studies we observed

that Rac GTPase signaling is also required for the overshoot phenotype in *cacn-1* RNAi animals. Loss of *ced-2*, *ced-5*, or *mig-2* strongly suppresses the *cacn-1* overshoot phenotype (Table 3). The *ced-10(n1993), cacn-1* RNAi animals are developmentally delayed relative to the other animals tested, and the DTCs often do not fully complete their migratory path by the time point these defects are scored (60 hours post hatching). It is therefore difficult to conclude that the DTC migration past the midline is specifically suppressed by *ced-10*. In addition, *pak-1* and *max-1* also appear to suppress the DTC overshoot in *cacn-1* RNAi animals, but this could be due to an increase in the percentage of DTCs undergoing extra turns. Therefore, we conclude that expression of *ced-2*, *ced-5*, and *mig-2* gene products are required for the DTC to continue migrating past the midline in *cacn-1* RNAi animals. Given these results, we speculated CACN-1 might normally function to suppress *mig-2* transcription in late L4 and adult animals. In order to investigate this idea, MIG-2::GFP animals (N=90) and CED-10::GFP animals (N=88) were treated with control RNAi or *cacn-1* RNA and visualized at 72 hours. No correlation between level of GFP expression and the RNAi treatment was observed. In addition, MIG-2::GFP levels were quantified in animals in which the DTC was clearly visible and not occluded by the intestine or developing embryos. MIG-2::GFP expression levels in the *cacn-1* RNAi treated animals did not differ significantly from controls. (Supplementary Fig. S2). These results suggest CACN-1 might not regulate *mig-2* (or *ced-10)* transcriptionally. This is consistent with our quantitative RT-PCR results showing *mig-2* transcript levels do not change significantly in *cacn-1* RNAi treated animals (data not shown). We predict that a function of *cacn-1* is to reduce activity of *mig-2* post-transcriptionally, which thereby leads to the cessation of DTC migration at the end of larval development.

Discussion

This study presents the first characterization of *C. elegans cacn-1*/*cactin*, a highly conserved novel regulator of developmental cell migration. We identified *cacn-1* in a genome-wide *in vivo* RNAi screen for cell migration genes (Cram et al., 2006). RNAi depletion experiments and analysis of the hypomorphic allele *cacn-1(tm3126)* demonstrate that CACN-1 is required for gonad morphogenesis. Strong expression of CACN-1 in the DTCs, and data from cell-specific RNAi depletion experiments, suggest CACN-1 is required cell-autonomously to control DTC migration. Importantly, our data suggest that CACN-1 acts specifically in the *mig-2*/Rac pathway, and in parallel to *ced-10*, to control DTC pathfinding.

We observed that reduction of *cacn-1* function leads to pathfinding defects, including wandering and supernumerary turns. These defects can be observed in N2 and *rrf-3* animals treated with RNAi during larval development, in the DTC-specific RNAi animals, and to some extent in *cacn-1(tm3126)* animals. In addition, the *cacn-1(tm3126)* animals provide a sensitized background in which earlier CACN-1 functions in DTC migration can be revealed. In *cacn-1 (tm3126)* animals treated with *cacn-1* RNAi, the DTCs often fail to migrate sufficiently along the ventral surface. It seems likely that *tm3126* protein has a shorter protein half-life than normal, rendering *cacn-1* RNAi either more effective, or effective earlier in development. These results suggest that some basal level of CACN-1 expression is required for DTC migration *per se*, but higher concentrations of the protein are required for proper response of the cell to guidance cues.

Although developmental control of cell migration is not completely understood, an emerging picture is that guidance receptors such as netrin (Killeen and Sybingco, 2008) and integrin (Vicente-Manzanares et al., 2009) orient cell direction by signaling through Rac family GTPases (Lundquist et al., 2001; Reddien and Horvitz, 2000). Rac GTPases are required for the migration of many types of cells and for axon pathfinding in many organisms (Lundquist, 2003; Ou and Vale, 2009). The *C. elegans* Racs CED-10 and RAC-2 are most similar to vertebrate Rac1, and MIG-2 is most similar to vertebrate RhoG (Lundquist, 2003). Despite the

name, phylogenetic analysis groups RhoG with the Rac GTPases, not with the Rho GTPases (Boureux et al., 2007). Although the precise function of RhoG in mammalian cells is not entirely clear, RhoG seems to play a role in Rac activation and Rac-regulated actin remodeling during cell migration (Katoh et al., 2006; Katoh and Negishi, 2003; Meller et al., 2008; van Buul et al., 2007). The MIG-2/RhoG homolog in Drosophila, Mtl, is required for axon guidance and branching (Hakeda-Suzuki et al., 2002). Downstream targets of Rac GTPase signaling include factors such as WAVE, WASP, ARP2/3, and cofilin (Shakir et al., 2008), which act directly to remodel the actin cytoskeleton. They also include the PAKs that, among other things, activate myosin to promote actin contractility (Arias-Romero and Chernoff, 2008; Lucanic and Cheng, 2008). Control of DTC migration by the Rac GTPases is complex. Both Rac gain and loss of function mutants lead to defects in DTC migration (Lundquist et al., 2001). Further complicating the situation is the partial genetic redundancy of *ced-10* and *mig-2* (and possibly, a third Rac, *rac-2)* in DTC migration. Disruption of both *ced-10* and *mig-2* Racs results in much more severe morphogenic defects and higher lethality (Lundquist et al., 2001). The DTC is not unique in this respect. In most cell types analyzed, highly homologous Rac GTPases are found to exhibit both cell-type specificity of function and partial genetic redundancy (Charest and Firtel, 2007; de Curtis, 2008; Heasman and Ridley, 2008). These results suggest that the correct level, or perhaps the controlled local activation of specific Rac GTPase signaling cascades, is required for migration of the DTC.

Our genetic interaction experiments suggest CACN-1 modulates Rac GTPase signaling to control DTC pathfinding. Specifically, we find that *cacn-1* RNAi significantly enhanced the *ced-10(n1993),* but not the *mig-2(mu28),* DTC pathfinding defects. These results suggest *cacn-1* is working in the same pathway as *mig-2*/Rac, and in parallel to *ced-10*/Rac to control DTC migration. Importantly, the specificity of this genetic interaction suggests *cacn-1* RNAi is not globally disrupting cell physiology. We also found that *cacn-1* acts genetically in parallel to both PAKs, *max-2* and *pak-1*. This fits in with previous results demonstrating that the PAKs are redundant as Rac GTPase effectors and can be activated by either Rac (Lucanic and Cheng, 2008).

In *cacn-1* RNAi animals, the DTC commonly fails to stop migrating at the correct point, far overshooting the midline. This is an intriguing phenotype, because very few genes that regulate DTC stopping are known. Our results demonstrate that the overshoot phenotype of *cacn-1* RNAi is suppressed by null mutations in *mig-2* and its upstream activators. This suggests MIG-2, CED-5 and CED-2 expression is required for the cell to continue migrating in the adult. A similar result was recently published in which joint RNAi knockdown of *ced-10* and *mig-2* strongly suppressed the failure-to-stop migration defect seen in *vab-3(e1796)* animals (Meighan and Schwarzbauer, 2007). This strongly suggests one function of CACN-1 may be to negatively regulate MIG-2 activity at the end of DTC migration. In addition, *cacn-1* RNAi enhances the very low overshoot phenotype in untreated *ced-2(n1994)* and *ced-5(n1812),* suggesting the presence of additional components functioning upstream of *cacn-1*.

CACN-1 is named after its fly homolog, Cactin, a Cactus/IKB interacting protein. Overexpression of Cactin enhances polarity defects in heterozygous *cactus* flies. The authors hypothesized Cactin may promote nuclear targeting of Dorsal/NFKB by destabilizing Cactus/IKB thereby leading to dorsal-ventral embryonic polarity defects (Lin et al., 2000). *C. elegans* is not thought to have a Dorsal/NFKB homolog, but it does have some of the signaling cascade including TOL-1/Toll like receptor, TRF-1/TRAF1, PLK-1/interleukin 1 receptor associated kinase, and IKB-1, an ankyrin repeat protein that shares some sequence homology with Cactus/IKB (Pujol et al., 2001). The *trf-1*, *plk-1* and *ikb-1*genes do not play any obvious role in cell migration or embryogenesis, but *tol-1* is required for body morphogenesis (Pujol et al., 2001). The potential connection between *cacn-1* and the *tol-1* pathway in *C. elegans* has not been investigated, and may be a fruitful area for future research. The results of our study

suggest, however, that *cacn-1* is required for developmental events including cell migration and gonad morphogenesis probably unrelated to the *tol-1* pathway.

Little is known about the biochemical function of CACN-1 or its homologs. The fly data suggests cactin may affect the expression, stability, or subcellular localization of ankyrin-repeat containing proteins. We are currently conducting a screen to identify proteins that interact biochemically with CACN-1. It is possible that this study will synergize with our genetic interaction results and provide direct evidence for the involvement of CACN-1 in Rac GTPase signaling, perhaps through direct interaction with MIG-2/Rac or with a Rac regulatory protein. Perhaps more likely, we may find that CACN-1 more generally affects cell polarity, indirectly altering the localization, stability, or localized activation of Rac or other signaling proteins. In either case, the striking sequence conservation of CACN-1 from worm to human suggests that elucidating the function of this protein is likely to improve our understanding of the fundamental regulation of cell migration during animal development.

Supplementary Material

Refer to Web version on PubMed Central for supplementary material.

Acknowledgments

Many *C. elegans* strains used in this work were provided by the *Caenorhabditis* Genetics Center, which is funded by the National Center for Research Resources, National Institutes of Health. We thank Alexander Bracey for help with *C. elegans* maintenance and Jean Schwarzbauer, Carol Warner, David Sherwood and Anne Hart for many helpful discussions. This work was supported by grant GM085077 from the National Institutes of Health to E.J.C.

References

Arias-Romero LE, Chernoff J. A tale of two Paks. Biol Cell 2008;100:97–108. [PubMed: 18199048]

Boureux A, Vignal E, Faure S, Fort P. Evolution of the Rho family of ras-like GTPases in eukaryotes. Mol Biol Evol 2007;24:203–216. [PubMed: 17035353]

Brenner S. The genetics of *Caenorhabditis elegans*. Genetics 1974;77:71–94. [PubMed: 4366476]

Charest PG, Firtel RA. Big roles for small GTPases in the control of directed cell movement. Biochem J 2007;401:377–390. [PubMed: 17173542]

Chen EB, Stern MJ. Understanding cell migration guidance: lessons from sex myoblast migration in *C. elegans*. Trends Genet 1998;14:322–327. [PubMed: 9724965]

Chen N, Harris TW, Antoshechkin I, Bastiani C, Bieri T, Blasiar D, Bradnam K, Canaran P, Chan J, Chen CK, Chen WJ, Cunningham F, Davis P, Kenny E, Kishore R, Lawson D, Lee R, Muller HM, Nakamura C, Pai S, Ozersky P, Petcherski A, Rogers A, Sabo A, Schwarz EM, Van Auken K, Wang Q, Durbin R, Spieth J, Sternberg PW, Stein LD. WormBase: a comprehensive data resource for *Caenorhabditis* biology and genomics. Nucleic Acids Res 2005;33:D383–389. [PubMed: 15608221]

Colavita A, Krishna S, Zheng H, Padgett RW, Culotti JG. Pioneer axon guidance by UNC-129, a *C. elegans* TGF-beta. Science 1998;281:706–709. [PubMed: 9685266]

Cram EJ, Shang H, Schwarzbauer JE. A systematic RNA interference screen reveals a cell migration gene network in *C. elegans*. J Cell Sci 2006;119:4811–4818. [PubMed: 17090602]

de Curtis I. Functions of Rac GTPases during neuronal development. Dev Neurosci 2008;30:47–58. [PubMed: 18075254]

Edgley MK, Baillie DL, Riddle DL, Rose AM. Genetic balancers. WormBook 2006 Apr;6:1–32. [PubMed: 18050450]

Hakeda-Suzuki S, Ng J, Tzu J, Dietzl G, Sun Y, Harms M, Nardine T, Luo L, Dickson BJ. Rac function and regulation during *Drosophila* development. Nature 2002;416:438–442. [PubMed: 11919634]

Hall A. Rho GTPases and the control of cell behaviour. Biochem Soc Trans 2005;33:891–895. [PubMed: 16246005]

Heasman SJ, Ridley AJ. Mammalian Rho GTPases: new insights into their functions from in vivo studies. Nat Rev Mol Cell Biol 2008;9:690–701. [PubMed: 18719708]

Hope, IA. C. elegans, A Practical Approach. Oxford University Press; Oxford: 1999.

Kamath RS, Fraser AG, Dong Y, Poulin G, Durbin R, Gotta M, Kanapin A, Le Bot N, Moreno S, Sohrmann M, Welchman DP, Zipperlen P, Ahringer J. Systematic functional analysis of the *Caenorhabditis elegans* genome using RNAi. Nature 2003;421:231–237. [PubMed: 12529635]

Katoh H, Hiramoto K, Negishi M. Activation of Rac1 by RhoG regulates cell migration. J Cell Sci 2006;119:56–65. [PubMed: 16339170]

Katoh H, Negishi M. RhoG activates Rac1 by direct interaction with the Dock180-binding protein Elmo. Nature 2003;424:461–464. [PubMed: 12879077]

Killeen MT, Sybingco SS. Netrin, Slit and Wnt receptors allow axons to choose the axis of migration. Dev Biol 2008;323:143–151. [PubMed: 18801355]

Kimble J, Hirsh D. The postembryonic cell lineages of the hermaphrodite and male gonads in *Caenorhabditis elegans*. Dev Biol 1979;70:396–417. [PubMed: 478167]

Lee M, Cram EJ, Shen B, Schwarzbauer JE. Roles for beta(*pat-3*) integrins in development and function of *Caenorhabditis elegans* muscles and gonads. J Biol Chem 2001;276:36404–36410. [PubMed: 11473126]

Lehmann R. Cell migration in invertebrates: clues from border and distal tip cells. Curr Opin Genet Dev 2001;11:457–463. [PubMed: 11448633]

Levy-Strumpf N, Culotti JG. VAB-8, UNC-73 and MIG-2 regulate axon polarity and cell migration functions of UNC-40 in *C. elegans*. Nat Neurosci 2007;10:161–168. [PubMed: 17237777]

Lin P, Huang LH, Steward R. Cactin, a conserved protein that interacts with the Drosophila IkappaB protein cactus and modulates its function. Mech Dev 2000;94:57–65. [PubMed: 10842059]

Lucanic M, Cheng HJ. A RAC/CDC-42-independent GIT/PIX/PAK signaling pathway mediates cell migration in *C. elegans*. PLoS Genet 2008;4(11):e1000269. [PubMed: 19023419]

Lundquist EA. Rac proteins and the control of axon development. Curr Opin Neurobiol 2003;13:384–390. [PubMed: 12850224]

Lundquist EA, Reddien PW, Hartwieg E, Horvitz HR, Bargmann CI. Three *C. elegans* Rac proteins and several alternative Rac regulators control axon guidance, cell migration and apoptotic cell phagocytosis. Development 2001;128:4475–4488. [PubMed: 11714673]

Meighan CM, Schwarzbauer JE. Control of *C. elegans* hermaphrodite gonad size and shape by *vab-3*/Pax6-mediated regulation of integrin receptors. Genes Dev 2007;21:1615–1620. [PubMed: 17606640]

Meller J, Vidali L, Schwartz MA. Endogenous RhoG is dispensable for integrin-mediated cell spreading but contributes to Rac-independent migration. J Cell Sci 2008;121:1981–1989. [PubMed: 18505794]

Merz DC, Zheng H, Killeen MT, Krizus A, Culotti JG. Multiple signaling mechanisms of the UNC-6/netrin receptors UNC-5 and UNC-40/DCC in vivo. Genetics 2001;158:1071–1080. [PubMed: 11454756]

Nishiwaki K. Mutations affecting symmetrical migration of distal tip cells in *Caenorhabditis elegans*. Genetics 1999;152:985–997. [PubMed: 10388818]

Ou G, Vale RD. Molecular signatures of cell migration in *C. elegans* Q neuroblasts. J Cell Biol 2009;185:77–85. [PubMed: 19349580]

Pujol N, Link EM, Liu LX, Kurz CL, Alloing G, Tan MW, Ray KP, Solari R, Johnson CD, Ewbank JJ. A reverse genetic analysis of components of the Toll signaling pathway in *Caenorhabditis elegans*. Curr Biol 2001;11:809–821. [PubMed: 11516642]

Qadota H, Inoue M, Hikita T, Koppen M, Hardin JD, Amano M, Moerman DG, Kaibuchi K. Establishment of a tissue-specific RNAi system in *C. elegans*. Gene 2007;400:166–173. [PubMed: 17681718]

Reddien PW, Horvitz HR. CED-2/CrkII and CED-10/Rac control phagocytosis and cell migration in *Caenorhabditis elegans*. Nat Cell Biol 2000;2:131–136. [PubMed: 10707082]

Rossman KL, Der CJ, Sondek J. GEF means go: turning on RHO GTPases with guanine nucleotide-exchange factors. Nat Rev Mol Cell Biol 2005;6:167–180. [PubMed: 15688002]

Scanlan MJ, Gordan JD, Williamson B, Stockert E, Bander NH, Jongeneel V, Gure AO, Jager D, Jager E, Knuth A, Chen YT, Old LJ. Antigens recognized by autologous antibody in patients with renal-cell carcinoma. Int J Cancer 1999;83:456–464. [PubMed: 10508479]

Shakir MA, Jiang K, Struckhoff EC, Demarco RS, Patel FB, Soto MC, Lundquist EA. The Arp2/3 activators WAVE and WASP have distinct genetic interactions with Rac GTPases in *Caenorhabditis elegans* axon guidance. Genetics 2008;179:1957–1971. [PubMed: 18689885]

Timmons L. Delivery methods for RNA interference in *C. elegans*. Methods Mol Biol 2006;351:119–125. [PubMed: 16988430]

van Buul JD, Allingham MJ, Samson T, Meller J, Boulter E, Garcia-Mata R, Burridge K. RhoG regulates endothelial apical cup assembly downstream from ICAM1 engagement and is involved in leukocyte trans-endothelial migration. J Cell Biol 2007;178:1279–1293. [PubMed: 17875742]

Vicente-Manzanares M, Choi CK, Horwitz AR. Integrins in cell migration--the actin connection. J Cell Sci 2009;122:199–206. [PubMed: 19118212]

Zipkin ID, Kindt RM, Kenyon CJ. Role of a new Rho family member in cell migration and axon guidance in *C. elegans*. Cell 1997;90:883–894. [PubMed: 9298900]

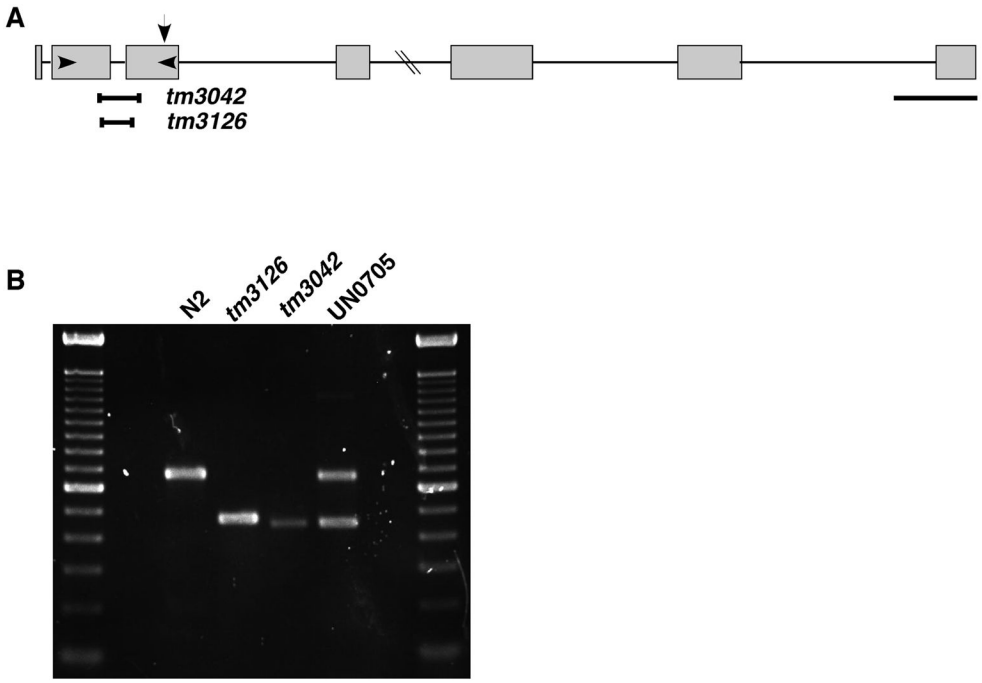

Fig. 1.

Analysis of *cacn-1* deletion alleles *tm3042* and *tm3126*. A) Diagrammatic representation of *cacn-1* gene structure. Brackets indicate DNA sequences deleted in *tm3042* and *tm3126*. Arrow indicates the position of a stop codon resulting from the *tm3042* allele. Arrowheads indicate the positions of PCR primers used in (B). Scale bar is 500 bp. Diagram is to scale except for intron 4, which is 3418 bp. B) PCR of genomic DNA from single wildtype (N2), mutant (*tm3126* and *tm3142*), and balanced mutant animals (UN0705) indicates the expected deletion sizes. DNA ladder indicates 100 bp intervals.

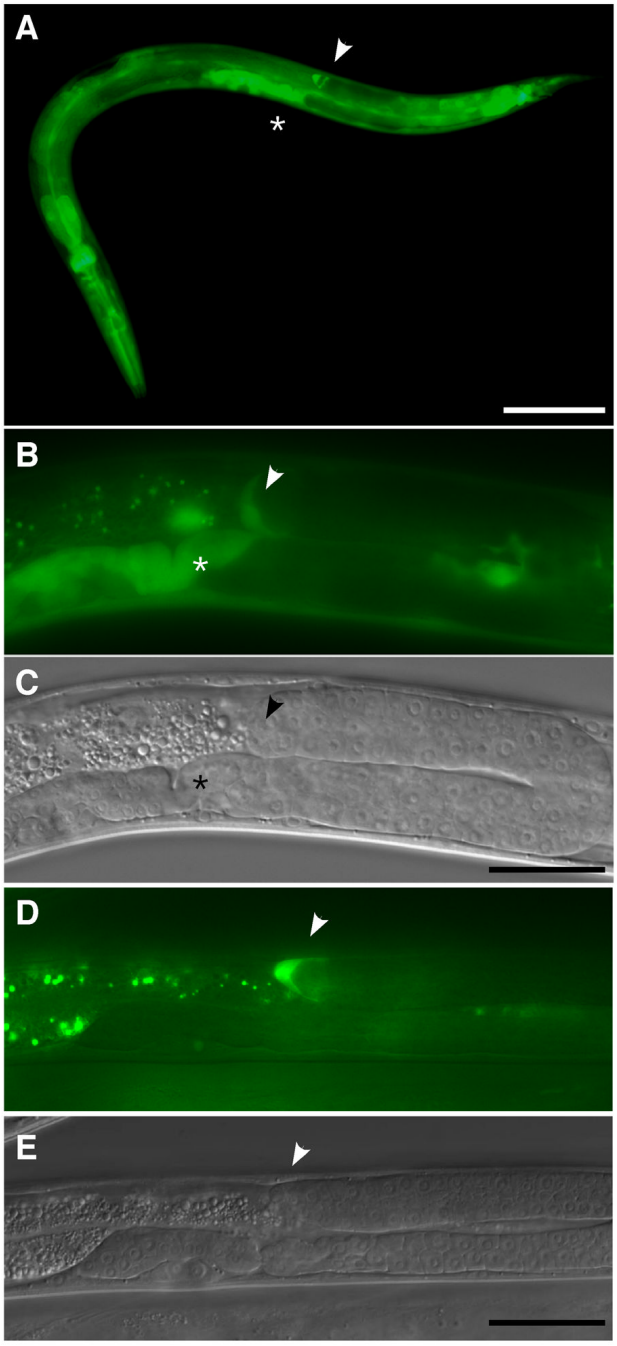

Fig. 2.

Expression pattern of the *cacn-1* promoter in L4 and adult wild-type hermaphrodites. The GFP expression pattern was examined by fluorescence microscopy of the *cacn-1p*::GFP(NK598) transcriptional reporter line. A) GFP is expressed in the pharynx, intestine, vulva, spermatheca (asterisk) and DTC (arrowhead). Scale bar 100 μm. B) DTC expression in the spermatheca (asterisk) and DTC (arrowhead) of an L4 animal, with matching DIC image (C). Scale bar 25 μm. D) Translational fusion *cacn-1* ::GFP expression throughout the DTC, with matching DIC image (E). Scale bar 25 μm.

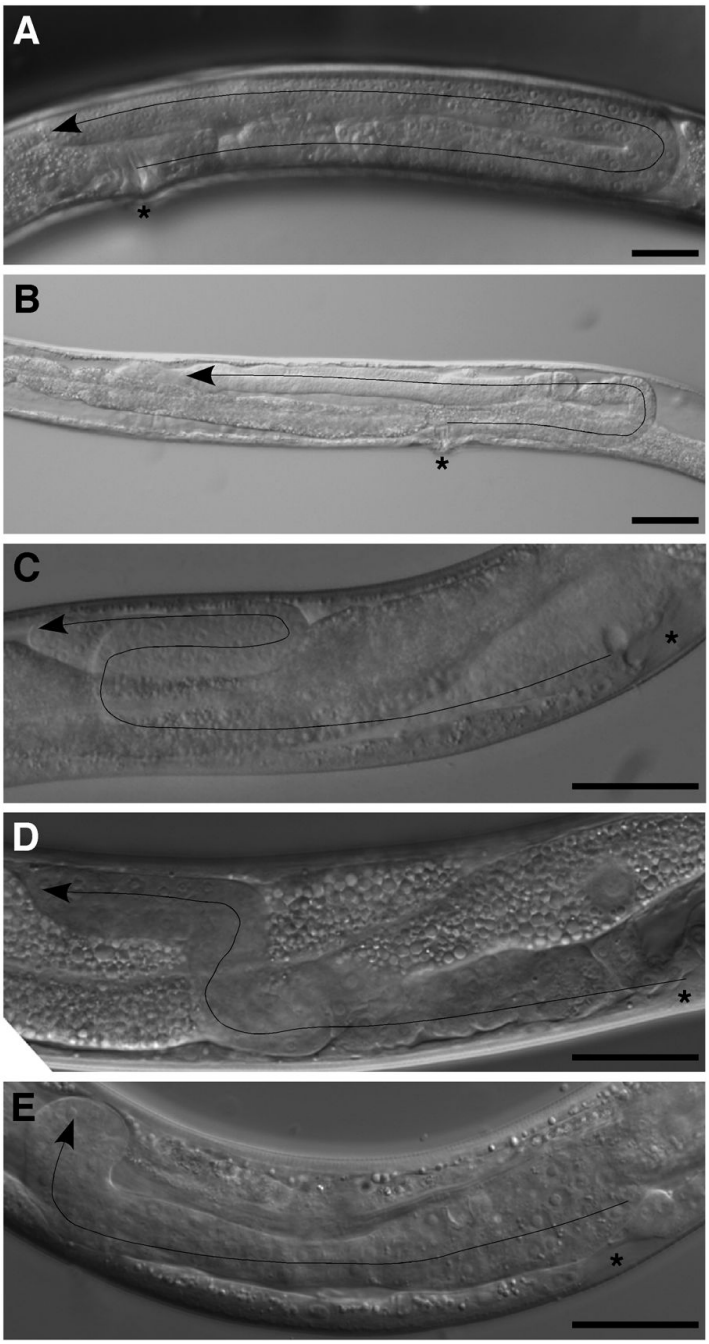

Fig. 3.

cacn-1 is required for correct DTC migration. RNAi sensitive *rrf-3(pk1426)* (AC) or *cacn-1 (tm3126)* (D, E) animals were grown on *E. coli* HT115(DE3) carrying empty vector (A, D) or *cacn-1* RNAi plasmid (B, C, E). Arrows indicate the path taken by the DTC as inferred from gonad shape in DIC images of L4 or young adult hermaphrodites. The position of each vulva is indicated by an asterisk. Scale bars are 50 μm (A, B) and 25 μm (C–E).

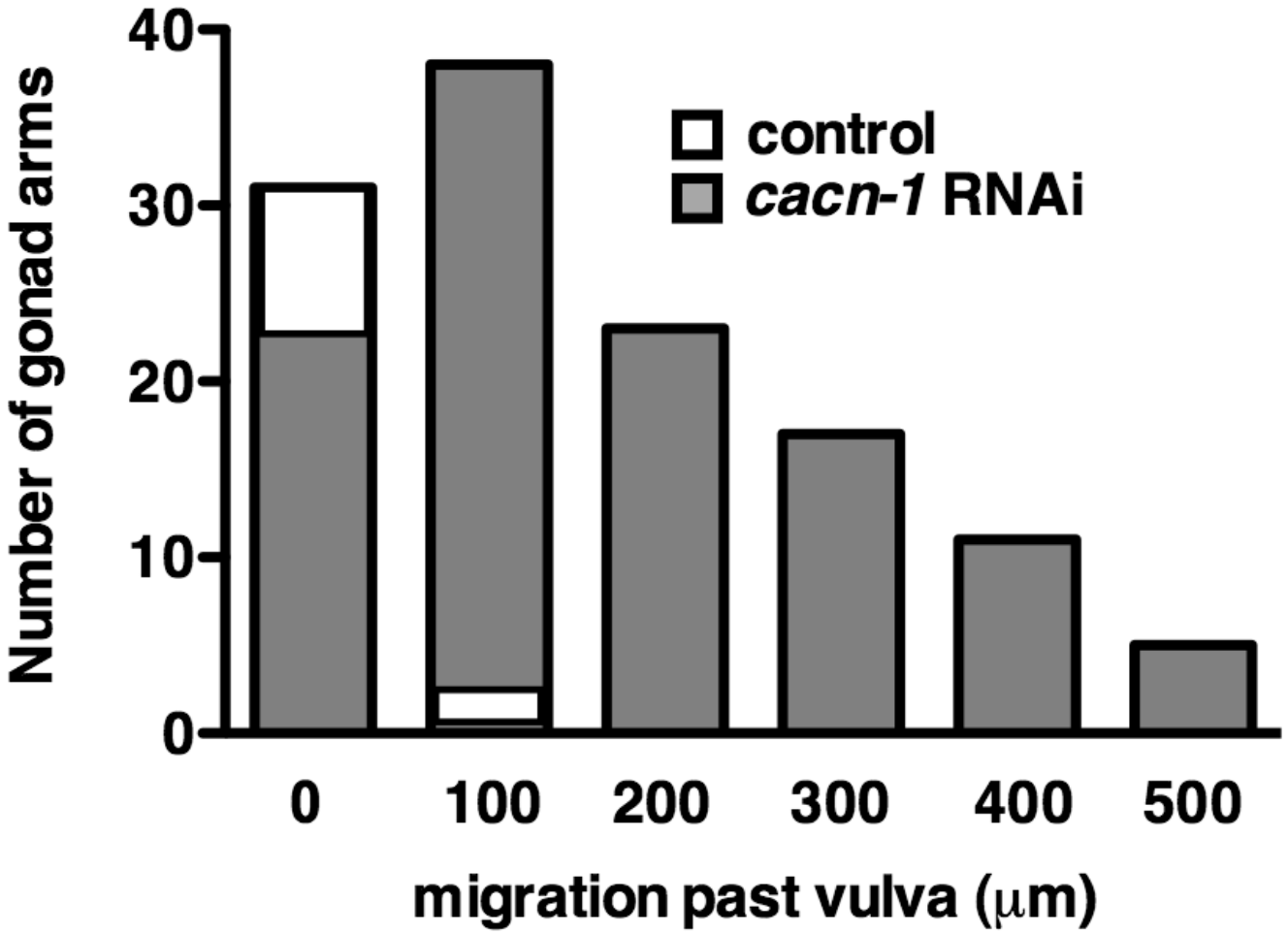

Fig. 4.

cacn-1 is required for cessation of DTC migration. RNAi sensitive *rrf-3 (pk1426)*animals were grown on *E. coli* HT115(DE3) carrying empty vector (white bars) or *cacn-1*RNAi plasmid (gray bars). Histogram indicates the number of distal tip cells that had traversedthe indicated distance past the vulva by 72 hours post egg lay.

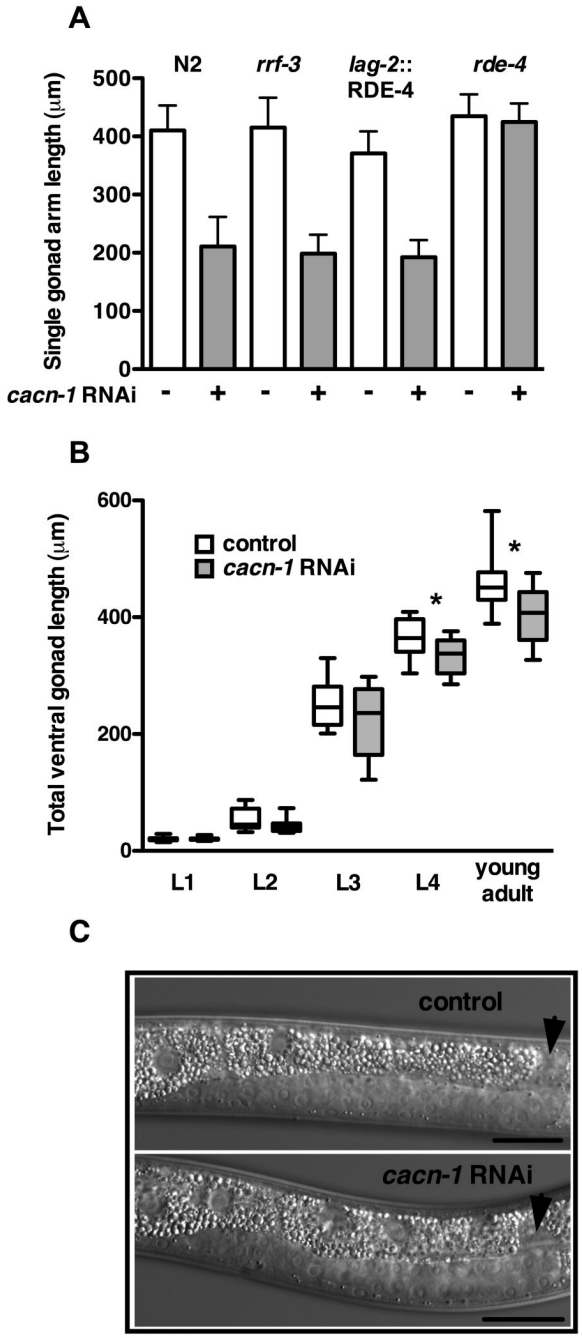

Fig. 5.

cacn-1 is required for gonad growth. Animals of the indicated genotypes were grown on *E. coli* HT115(DE3) carrying empty vector (white) or *cacn-1*RNAi plasmid (gray). A) Columns indicate the ventral extension of the gonad arm from the vulva to the first turn at 72 hours post egg lay. Error bars indicate the s.d. B) The box and whisker plot indicates the total ventral length of the gonad at the indicated developmental stage. The line indicates the median and the box represents data from the middle two quartiles. The whisker encompasses data from the outer two quartiles. A significant difference between control and *cacn-1*RNAi is observed only in L4 (p=0.02 Mann-Whitney test) and adult (p=0.002) animals. C) Treatment with *cacn-1* RNAi does not disrupt the timing of the ventral to dorsal turn. DIC images of L3 *rrf-3*

(pk1426) animals fed control (top panel) or *cacn-1* RNAi (bottom panel). Arrowhead indicates the position of the DTC, which has just navigated the first turn. Scale bar 25 μm.

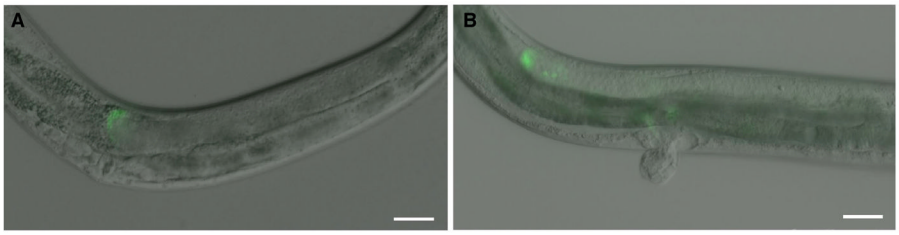

Fig 6.

cacn-1 is required within the DTC. DTC-specific RNAi animals *rde-4(ne3010)*; [*lag-2*::RDE-4::GFP] were grown on *E. coli* HT115(DE3) carrying empty vector (A) or *cacn-1* RNAi plasmid (B). GFP signal indicates the position of the DTC. Scale bars A) 20 μm, B) 25 μm.

Table 1

ired for correct migration of the DTC.

	N	*cacn-1* RNAi	extra turn[Ψ]	wandering[¥]	overshoot[ɔ#]	other[π]
	337	–	0%	0%	0%	0%
	361	+	3%	7%	33%	0%
	154	–	0%	3%	1%	0%
	168	+	17%	7%	43%	8%
	450	–	6%	4%	1%	3%
	118	+	13%	12%	10%	54%
(tm3042)	134	–	4%	30%	8%	4%
/+	170	–	1%	8%	9%	1%

scored in young adults, 48 hours and 72 hours post egg-prep, using Nomarski microscopy.

ad arm with extra turns in the migration pathway after the dorso-ventral turn. Anterior is left, dorsal is upwards. The distal tip cell is shown in black.

h wandering dorsal migration were scored.

hat failed to stop at the midline leading to an overshooting gonadal arm was observed.

t stopped migrating, exhibited mild defects during the dorso-ventral turn, or lacked an intact gonad arm structure were categorized as ‘other’.

Table 2

mously in the DTC.

	N	RNAi	 extra turn	 wandering	 overshoot	 no migration
	337	control	0%	0%	0%	0%
	154		0%	3%	1%	0%
	165		0%	4%	1%	0%
-6]	134		0%	2%	1%	0%
-6]	86		0%	1%	0%	0%
	361	*cacn-1*	3%	7%	33%	0%
	168		17%	7%	43%	3%
	82		0%	0%	0%	0%
-6]	109		2%	6%	40%	0%
-6]	124		0%	2%	0%	0%
	230	*gon-1*	0%	0%	0%	99%
	46		0%	0%	0%	100%
	132		0%	2%	2%	0%
-6]	72		0%	0%	1%	94%
-6]	112		0%	1%	0%	2%

ed in *cacn-1* RNAi and control RNAi treated young adults, 48 hours post egg-prep.

which causes a prominent DTC migration defect in wild type animals. The *rde-4(ne301)* animals are not sensitive to RNAi.

xpression in the DTC. RNAi depletion was specific to cells expressing *lag-2*::RDE-4::GFP

the intestine. Treatment with *cacn-1* RNAi and *gon-1* RNAi showed minimal, if any, spreading of RNAi from the intestine.

o migrate were observed in *gon-1* RNAi treated animals.

Table 3

etically with Rac signaling.

N	*cacn-1*RNAi	extra turn	wandering	overshoot	no migration
76	–	0%	2%	0%	0%
14	+	12%	19%	62%**	0%
72	–	21%	5%	1%	4%
60	+	39%*	3%	1%	11%
02	–	18%	6%	0%	0%
54	+	11%	5%	19%	0%
52	–	2%	12%	0%	0%
72	+	22%*	7%	19%	0%
50	–	26%	2%	0%	0%
70	+	29%	3%	26%	0%
06	–	17%	3%	2%	0%
28	+	23%	9%	15%	0%
70	–	38%	5%	2%	0%
36	+	43%	4%	13%	1%
16	–	0%	3%	0%	0%
08	+	17%	6%	39%	0%
40	–	1%	4%	1%	0%
94	+	22%	9%	46%	0%
10	–	3%	8%	20%	0%
02	+	25%*	14%	37%	0%
46	–	2%	18%	13%	0%
38	+	35%*	6%	22%	0%

scored for DTC migration defects.

ignificantly increased in N2, *ced-10(n1993)*, *ced-10(n3417)/+*, *pak-1(ok448)*, *pak-1(tm403)*, *max-2(nv162)*, and *max-2(cy2)* animals when treated with *cacn-1* RNAi (shaded boxes).
ed on non-overlapping 95% confidence intervals) in the extra turn phenotype in mutant *cacn-1* RNAi treated animals compared to N2 *cacn-1* RNAi treated animals are indicated
tion of DTCs that failed to stop, thereby overshooting the midline, was significantly increased in N2, *mig-2 (mu28)*, *ced-10(n3417)/+*, *ced-2(n1994)*, *ced-5(n1812)*, *pak-1(ok448)*,

and *pak-1 (tm403)* animals treated with *cacn-1* RNAi (shaded boxes). However, in all cases, the proportion of DTCs failing to stop in the mutant animals is significantly reduced compared to N2 animals treated with *cacn-1* RNAi (**).